Many-body transverse interactions in the quantum annealing of the p-spin ferromagnet

Beatriz Seoane

Departamento de Física Teórica I, Universidad Complutense, 28040 Madrid, Spain.
Instituto de Biocomputación y Física de Sistemas Complejos (BIFI), Zaragoza, Spain.

E-mail: beatriz.seoane@fis.ucm.es

Hidetoshi Nishimori

Department of Physics, Tokyo Institute of Technology, Oh-okayama, Meguro-ku, Tokyo 152-8551, Japan

Abstract. We study the performance of quantum annealing for the simple p-body infinite-range ferromagnetic Ising model. In particular, we generalize the transverse antiferromagnetic interactions proposed by Seki and Nishimori as a quantum driver to many-body transverse interactions to understand if the two-body interactions are essential to allow the system to avoid troublesome first-order quantum phase transitions. We conclude that the general many-body interactions are effective to let the system evolve only through second-order transitions as long as a few minor conditions are satisfied. It is also discussed whether the overlap of the ground-state wave function of the new driver term with the target ground state is an essential factor for the success.

1. Introduction

The task of finding the configuration that optimizes a given cost or energy function $\mathcal{H}(\{S_i\})$ dependent on a large number N of variables $S_1, \ldots, S_N$ (often subjected to constraints) is a whole research field by itself, common to many fields in science. Finding the minimum energy or cost often becomes a hard task when the constraints in the system, or the interactions between variables, induce frustration because there is no way to find a minimum configuration that minimizes the problem locally. The frustration leads to a rugged landscape of many relative minima, and an exhaustive search for the absolute minimum is just not feasible for the interesting sizes (the dimension of the system often grows exponentially with N). As examples of these optimization problems, one can cite the traveling sales problem [1] or the k-SAT problem [2] in computer science, or finding the ground state of spin glass in physics [3, 4].

Complexity in optimization problems is commonly classified as P if an algorithm is known to solve the problem in a time that grows polynomially with N. On the contrary, if it is not the case, and the time scales faster with N, these problems are labeled NP and considered as hard problems. Among all the NP problems, there is a subgroup named NP complete so that any possible NP problem can be reduced to one of them by means of a polynomial algorithm. Thus, if one algorithm were found that solved polynomically an NP complete problem, the whole family of problems would also become easy. The problems mentioned above belong all to the NP-complete class.‡

Statistical mechanics, based on physical intuition, has contributed a lot in the development of new strategies for optimization problems: parallel tempering or replica exchange [6], and simulated annealing [7] are the two popular and widely used examples. In this last method, fluctuations are introduced in the problem through a ficticious temperature. This temperature favors the jump over barriers and thus encourages the system to visit other possible minima. The system is then simulated at a temperature $T(t)$ that decreases slowly with time until it is finally switched off at the end of the simulation. We will refer to this simulated annealing as classical annealing (CA) in contrast to the quantum annealing (QA) [8, 9, 10, 11], where fluctuations are induced also in the system but this time quantum ones. Quantum perturbations allow tunneling effects, and thus, if narrow enough, barriers can be crossed instead of surpassed.

In the traditional QA formulation, a time-dependent Hamiltonian is introduced

$$\hat{H}(t) = s(t)\hat{H}_0 + [1 - s(t)]\,\hat{V}, \tag{1}$$

where $\hat{H}_0$ is the target Hamiltonian (or the cost function that one wants to minimize) and $\hat{V}$ represents the quantum perturbations. In the field we are working in, the Hamiltonian $\hat{H}_0$ represents the magnetic interaction between spins. For the sake of simplicity, we will consider that $\hat{H}_0$ only depends on the z components of the Pauli matrix $\hat{\sigma}_i^z$, where $i(= 1, \ldots, N)$ labels the index of each spin in the system. As normally, we are interested

‡ With the exception of the 2-SAT problem and the $2D$ Ising spin glass [5] that can be solved polynomically.

in finding the lowest energy spin configuration, i.e. the ground state. Now we introduce the quantum fluctuations through a spin driver term $\hat{V}$. In principle, this term is arbitrary, as long as it does not commute with $\hat{H}_0$. In addition, we impose that $\hat{V}$ has a single, trivial ground state. A typical example of a driver Hamiltonian is the transverse-field operator

$$\hat{V}_{\mathrm{TF}} \equiv -\sum_{i=1}^{N} \hat{\sigma}_i^x, \tag{2}$$

where the $\hat{\sigma}_i^x$ $(i = 1, \ldots, N)$ are the x components of the Pauli matrix. This perturbation is very intuitive, since it represents nothing but the interaction with a magnetic field along the x direction that induces quantum transitions between the eigenstates of $\hat{\sigma}_i^z$, whose modulus is tuned through the control parameter $s(t)$. Initially, at $t = 0$, the control parameter $s(t)$ starts at $s(0) = 0$, with $\hat{H}(0) = \hat{V}$, and increases monotonically with time until it reaches unity at time τ and $\hat{H}(\tau) = \hat{H}_0$. Let us choose the simplest possible scheme where the control parameter grows linearly with time, i.e. $s(t) = t/\tau$.

The evolution of the system, $|\Phi(t)\rangle$, is determined by the Schrödinger equation,

$$\mathrm{i}\frac{\mathrm{d}}{\mathrm{d}t}\,|\Phi(t)\rangle = \hat{H}(t)\,|\Phi(t)\rangle\,,\ 0 \leq t \leq \tau. \tag{3}$$

The initial state $|\Phi(0)\rangle$ is the ground state of the driver Hamiltonian $\hat{V}$ and is thus known. If the parameter $s(t)$ is changed very slowly (τ is very long), the state will be at every time very close to the instantaneous ground state. If it so, by tuning the parameters, one will move adiabatically from the initial ground state to the ground state of $\hat{H}_0$.

The adiabatic theorem states that the system stays close to the instantaneous ground state as long as $\tau \gg \Delta_{\mathrm{min}}^{-2}$ where Δ_{min} is the minimum energy gap from the ground state. Of course, in order for the above argument to be of general use, this Δ_{min} cannot decrease with N too fast. In fact, if the energy gap decays exponentially with the system size, as happens generally in first-order transitions, the running time will increase exponentially with N and the QA would not help to solve the problem efficiently.

This vanishing exponential gap present in many first-order transitions is sometimes considered to be one of the most important drawbacks of quantum annealing. Its presence was somehow shadowed for certain time by the preasymptotic behavior displayed in the small system sizes feasible in simulations [12, 13, 14]. Indeed, in the last years, an increasing number of first-order transitions in the annealing parameters are being found [15, 16, 17, 18, 19]. It has thus been suggested that the presence of these quantum first-order transitions when tuning the transverse field is an intrinsic property of the systems with complicate free energy landscape, i.e. the hard problems, leading a pessimistic scenario for the QA algorithm [15, 16, 17, 18, 19].

Recently, it was found that the ferromagnetic p-spin model, a model without disorder and with a simple free energy landscape, also suffers from this kind of first-order transition [18]. Due to its simplicity, this model constitutes a perfect benchmark

to study the QA performance. Indeed, it was recently shown [20] that, at least for finite values of p and $p \neq 3$, it is possible to avoid this first-order transition by appending an additional antiferromagnetic driver term and performing the annealing along a curve in a space of two annealing parameters instead of just one. This study changes the paradigm about first-order transitions in QA, since the failure of QA strategies observed up to now could be a failure of the standard formulation of QA with a transverse field, not a failure of the algorithm itself.

Here we go deeper into this problem, studying a family of alternative driver terms, displaying different symmetries. We show analytically the existence of paths that cross only a second-order transition and thus the speed of QA is not exponentially damped. Indeed, in a second order transition the gap vanishes only polinomially with the number of particles, which must be compared with the exponential damping observed in the first order transition. The solution to the problem is not unique and we study the properties of these new driver terms, reaching the conclusion that the structure of the ground state of the additional Hamiltonians is not the main important feature that makes the whole algorithm success as argued in [21].

2. Problem

Our starting point is the ferromagnetic p-spin model ($p = 2, 3, 4 \ldots$)

$$\hat{H}_0 = -N \left(\frac{1}{N} \sum_{i=1}^{N} \hat{\sigma}_i^z \right)^p . \tag{4}$$

The ground state for this model, $|\Phi_0\rangle$, corresponds to the state of all the spins aligned along the z direction. In order to avoid the degeneracy of the up and down configurations present in even powers of p, we consider here only the odd values of p and $p \geq 3$. In the limiting $p \to \infty$ case, this model is nothing but the Grover problem [18, 22]. Although the Grover's quantum algorithm, whose reformulation in quantum annealing is given in [23], is considered a success of the quantum algorithm (provides a square-root gain with respect to the classical search [24]) it remains being a hard problem even with quantum algorithms. Now we consider the problem of finding this already known ground state $|\Phi_0\rangle$ of (4) with the QA algorithm using two driving terms.

As usual, we consider the traditional transverse field operator,

$$\hat{V}_{\mathrm{TF}} \equiv -\sum_{i=1}^{N} \hat{\sigma}_i^x, \tag{5}$$

whose ground state, $\left|\Phi^{\mathrm{TF}}\right\rangle$, is the one where all the N spins are pointing to the positive direction along the x axis. We next introduce a second Hamiltonian inspired in the antiferromagnetic interaction suggested in [20],

$$\hat{V}_k = +N \left(\frac{1}{N} \sum_{i=1}^{N} \hat{\sigma}_i^x \right)^k , \tag{6}$$

that depends on a parameter $k(>1)$. When $k=2$, we recover the antiferromagnetic interaction studied in [20]. The ground state for this Hamiltonian, namely $|\Phi_k\rangle$, depends on the value of the power k. When k is odd, the energy is minimum when all spins are aligned along the x axis but pointing to the negative direction. On the contrary, when k is even, the ground state corresponds to the state with total $\sum_{i=1}^{N}\sigma_i^x=0$ if N is odd, or $\sum_{i=1}^{N}\sigma_i^x=\pm 1$ for N even. One of the goals of the present paper is to clarify whether the value $k=2$ is essential to avoid the first-order transition.

If we sum up (1), (5) and (6), the new Hamiltonian of the problem reads as

$$\hat{H}(s,\lambda)=s\left[\lambda\hat{H}_0+(1-\lambda)\hat{V}_k\right]+(1-s)\hat{V}_{\rm TF}. \tag{7}$$

Here there are two annealing parameters, s and λ. These parameters will be tuned slowly during the annealing process so that, at the final time, τ, $s(\tau)=\lambda(\tau)=1$ and the target Hamiltonian (4) is thus recovered. In that way, one can explore the annealing process following infinitely different paths. It might resemble the idea of nondeterministic Turing machines, but one must always keep in mind that, even though many paths are possible, only one is chosen in each particular realization.

The traditional QA is one of the infinite possible paths in (7). In fact, one can remove the influence of $\hat{V}_k$, just by fixing $\lambda(t)=1$. Then, the annealing is performed by tuning s from 0 to 1. If one looks at the configurations, at $t=0$ all spins should be aligned with the x axis, and at the end, with the z axis. In this case, we know that the system suffers from a quantum first-order phase transition between these two states. This transition ruins the efficiency of the algorithm as it becomes exponential [18]. The idea of introducing this two-parameter space (λ,s) is precise to try avoid this transition by following an alternative route. Seki and Nishimori succeeded in finding ingenious paths [20] with antiferromagnetic interactions, and here, we generalize that method to check how the value of k affects the conclusion.

3. Analysis by a semi-classical approach

The QA strategy will succeed if we are able to find a path in the space of parameters (λ,s) that avoids crossing any first-order transition. With this aim, we compute in this section the phase diagram correspondent to the new Hamiltonian (7), as a function of the parameter k. The $N\to\infty$ limit can be computed analytically using a semi-classical approximation (method to be explained below) or the Trotter-Suzuki decomposition formula [25] and the static approximation (see Appendix A), leading to equivalent results.

3.1. General Properties

As a starting point, let us rewrite the Hamiltonian (7) in terms of the total spin variables ($S^\alpha=\frac{1}{2}\sum_{i=1}^{N}\sigma_i^\alpha$ with $\alpha=x$, y and z),

$$\hat{H}(s,\lambda)=-s\lambda N\left(\frac{2}{N}S^z\right)^p+s\,(1-\lambda)N\left(\frac{2}{N}S^x\right)^k-2(1-s)S^x. \tag{8}$$

This Hamiltonian commutes with the total squared spin, S^2. Since the total spin is conserved and the initial state in the annealing process is the one with all spins aligned with the x axis, we are only interested in studying the maximum possible S value, i.e. $S = N/2$.

Now, consider the normalized variables $m^\alpha = S^\alpha/S$, with $\alpha = x$, y and z. The commutation relations for these variables are

$$[m^x, m^y] = \mathrm{i}\frac{2}{N}m^z, \tag{9}$$

and cyclic permutations. The normalized variable m^α can take $N+1$ values within the interval $[-1, 1]$. Thus, in the large N limit, these variables commute, and we can consider them as the components of a classical unit vector, i.e. $\boldsymbol{m} = (\cos\theta, \sin\theta\sin\varphi, \sin\theta\cos\varphi)$, being θ the polar angle measured from the x axis, and φ the azimuthal one measured from the z axis.

Considering the system now as classic, we can write the energy per spin as

$$e = -s\lambda(\sin\theta\cos\varphi)^p + s\,(1-\lambda)\cos^k\theta - (1-s)\cos\theta. \tag{10}$$

The equilibrium state will be determined by the minimum of e. Since p is odd, the minimum lies on the plane with $\varphi = 0$, which we call XZ^+ plane. The energy on this plane is labeled only by the polar angle θ

$$e = -s\,\lambda\sin^p\theta + s\,(1-\lambda)\cos^k\theta - (1-s)\cos\theta. \tag{11}$$

We search the $\theta_0 \in [0, \pi]$ that minimizes (11)§. The condition for the minimum is

$$\frac{\partial e}{\partial\theta_0} = -p\,s\,\lambda\sin^{p-1}\theta_0\cos\theta_0 - k\,s\,(1-\lambda)\cos^{k-1}\theta_0\sin\theta_0 + (1-s)\sin\theta_0 = 0, \tag{12}$$

whose solutions are the angles θ_0 that satisfy either $\sin\theta_0 = 0$ or

$$p\,s\,\lambda\sin^{p-2}\theta_0\cos\theta_0 + k\,s\,(1-\lambda)\cos^{k-1}\theta_0 - 1 + s = 0. \tag{13}$$

These two equations have more than one solution, and each one corresponds to a different phase. We will consider them as ferromagnetic if $m^z(=\sin\theta_0) > 0$, and quantum paramagnetic if $m^z = 0$. The most stable one at each point (λ, s) will be the absolute minimum of e.

We begin with the quantum paramagnetic solutions. The equation $\sin\theta_0 = 0$ is satisfied for $\theta_0 = 0$ or π. The case $\theta_0 = 0$ corresponds to positive x magnetization, $m^x = 1$. We name this phase QP^+. Its energy is obtained by inserting this angle in (11),

$$e_{\mathrm{QP}^+}(s, \lambda) = s(1-\lambda) - 1 + s. \tag{14}$$

The other paramagnetic solution, $\theta_0 = \pi$, corresponds to negative magnetization, $m^x = -1$. We call this phase QP^-. This phase is only stable for odd values of k and its energy is

$$e_{\mathrm{QP}^-}(s, \lambda) = -s(1-\lambda) + 1 - s. \tag{15}$$

§ Negative magnetizations along z axis have always higher free energy due to the change of sign in the $\sin^p\theta$ term in (11) (remember that we only consider the p odd case in this work).

This phase will not appear in the phase diagrams for k even, since its energy is always positive in the range of parameters $0 \leq s,\, \lambda \leq 1$.

We consider next the ferromagnetic solutions ($\theta_0 > 0$). The purely ferromagnetic solution $\sin\theta_0 = 1$ is only a valid solution on the line $s = 1$. Apart from this line, equation (13) cannot be explicitly solved for any value of p, but it can be done in the $p \to \infty$ limit. We study below all the solutions for this limit and discuss their validity for p finite.

3.2. Phase diagram for $p \to \infty$

In this limit, (13) has two possible ferromagnetic solutions. The parameter p appears in (13) through $p \sin^{p-2}\theta_0$. We consider the two possible limits for the sine power, $\sin^{p-2}\theta_0 \to 1$ (for the F phase) and 0 (for the F' phase), always keeping $\theta_0 > 0$.

We begin the discussion with the F phase. With this aim, we assume

$$\sin^p \theta_0 \to 1, \tag{16}$$

and substitute it in (13),

$$p\, s\, \lambda \cos\theta_0 + k\, s\, (1-\lambda) \cos^{k-1}\theta_0 - 1 + s = 0. \tag{17}$$

In the $p \to \infty$ limit, this equation can only be satisfied if either the cosine vanishes, i.e. $\theta_0 = \pi/2$ (but only on the line $s = 1$), or $p \cos\theta_0$ tends to a constant. Let us investigate this second case. We consider $\cos\theta_0 = c/p$, with c a p-independent constant, and introduce it in (17), and taking the $p \to \infty$ limit, the equation reads

$$s\, \lambda\, c - 1 + s = 0, \tag{18}$$

whose solution is $c = (1-s)/s\lambda$. Thus,

$$\cos\theta_0 = \frac{1-s}{s\, p\, \lambda} \to 0, \tag{19}$$

is a solution to (13). Still we need to check that this θ_0 agrees with the initial assumption (16). Indeed,

$$\lim_{p\to\infty} \sin^{p-2}\theta_0 = \lim_{p\to\infty} \left[1 - \left(\frac{1-s}{2\, s\, p\, \lambda}\right)^2\right]^p = 1.$$

We obtain the energy for this phase introducing (19) in (11)

$$e_{\rm F}(s,\lambda)^k\big|_{p\to\infty} = -s\, \lambda. \tag{20}$$

On the other hand, the F' solution is obtained assuming the opposite limit,

$$p \sin^p \theta_0 \to 0. \tag{21}$$

Under this assumption, (13) reduces to

$$k\, s\, (1-\lambda) \cos^{k-1}\theta_0 - 1 + s = 0, \tag{22}$$

whose solution is

$$\cos\theta_0 = \left[\frac{1-s}{k\, s\, (1-\lambda)}\right]^{\frac{1}{k-1}}. \tag{23}$$

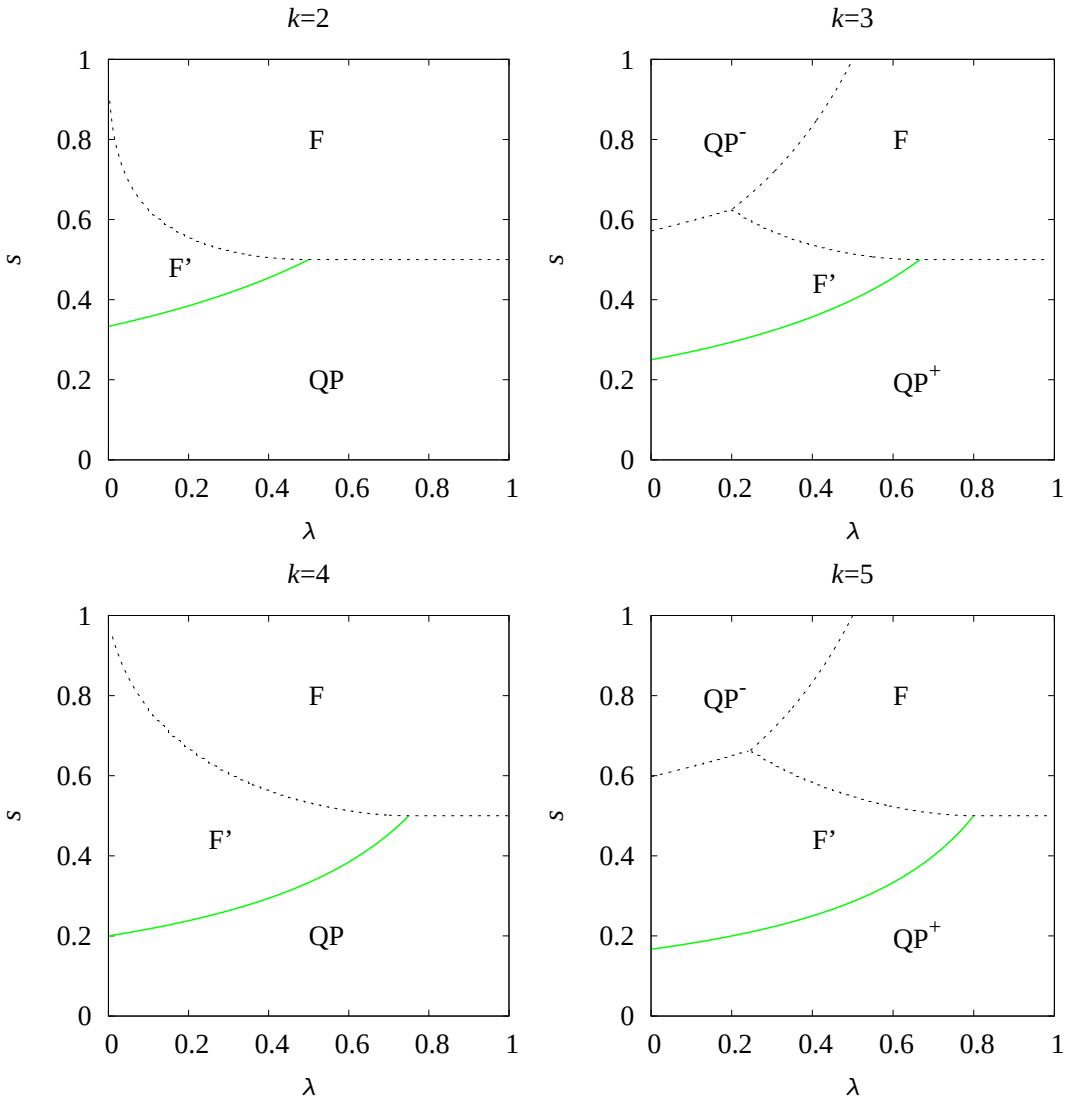

Figure 1. Phase diagram for $p \to \infty$. Dashed black lines represent first-order transitions, whereas the solid line in light green accounts for the second-order transition.

Note that if k is odd, the negative solution for the cosine is also a valid solution. However, it has always higher energy than its positive counterpart, so we will not consider it for further discussions.

The energy for the F' phase when $p \to \infty$ is

$$e_{\mathrm{F}'}(s,\lambda)\big|_{p\to\infty} = -\frac{k-1}{k}\left[\frac{1-s}{k\,s\,(1-\lambda)}\right]^{\frac{1}{k-1}}(1-s). \tag{24}$$

Up to this point, we have obtained all the possible solutions to (13) in the $p \to \infty$ limit: three (for even k) and four (for odd k) phases. We can use the energies to determine which phase is the most stable at each point (λ, s). We show in figure 1 several phase diagrams for $k = 2$, 3, 4 and 5. Let us analyze the nature of each transition. We begin with the transition line between the F' and QP^+ phases. This

line is obtained by solving $e_{\mathrm{F}'} - e_{\mathrm{QP}} = 0$ using the expressions (24) and (14). This equality is fulfilled on the line $s = 1/[1 + k(1 - \lambda)]$. On this line, $m^x = \cos\theta_0 = 1$ in both phases, which corresponds to a second-order transition. On the other hand, the transition between the F and the QP^+ phases lies on the $s = 1/2$ line and, since magnetization is discontinuous, it is first-order. The second-order transition extends from $(\lambda, s) = (0, 1/(k+1))$ to $(\lambda, s) = ((k-1)/k, 1/2)$, the point where these two kinds of transitions cross. According to that, the higher k is, the broader the second-order line and the smaller the QP^+ region are. Furthermore, in the $k \to \infty$ limit, the QP^+ region completely disappears.

Still there is a first-order transition between the F and F' phases, determined by the solution of $e_{\mathrm{F}'} - e_{\mathrm{F}} = 0$ using (24) and (20). We solve this equation numerically and obtain the curve displayed in figure 1. On this line, the magnetizations are discontinuous but at the point $(\lambda, s) = (0, 1)$ where they two become equal, $m^z = \sin\theta_0 = 1$. The transition is then first-order, but in the mentioned point, where it would be second-order.

Up to this point, the discussion is common for even and odd values of k. However, in this latter case the QP^- phase also exists. Thereby, two additional transitions between F or F' phases and the QP^- phase appear. In both cases the x magnetization changes the sign on the transition, and then, they are first-order. The transition lines are obtained by solving the equations $e_{\mathrm{QP}^-} - e_{\mathrm{F}} = 0$, leading to $s = 1/(2(1-\lambda))$, and $e_{\mathrm{QP}^-} - e_{\mathrm{F}'} = 0$ which must be solved numerically. We display all the transition lines in figure 1.

According to these results, when we consider the $p \to \infty$ limit, there is only one single path that succeeds in avoiding first order transitions. This is the straight line that joins the initial point $(\lambda, s) = (0, 0)$ with the left upper corner, $(0, 1)$, and the final state $(1, 1)$. However, even though this path only crosses second order transitions, along this way there is no quantum annealing process, as can be seen by an insertion of these parameter values into the Hamiltonian (7), and thus this path is meaningless.

4. Phase Diagram

The phase diagram for finite p is different. Now, there appear regions where first-order transitions disappear, leaving more space for annealing trajectories. We display the corresponding diagrams in figures 2, 3, 4 and 5 for $k = 2$, 3, 4 and 5, respectively. Again, the shape of the phase diagram strongly depends on whether k is even or odd. In the former, there are only three phases and in the latter the extra QP^- phase appears. Besides, the higher k is, the longer is the second-order transition line.

The picture of the ferromagnetic phase for finite p is rather complicated. When one solves numerically (13) and looks at the $\theta_0 > 0$ solutions, the situation is the following: in a wide region, one finds two possible alternative solutions that look very much alike to the F and F' phases discussed for the $p \to \infty$ limit. However, near the left and upper corner in the phase diagram, there is one single ferromagnetic solution which is neither F nor F' but something intermediate. In fact, for k even, one can find paths through which the magnetization evolves continuously from the F' to the F

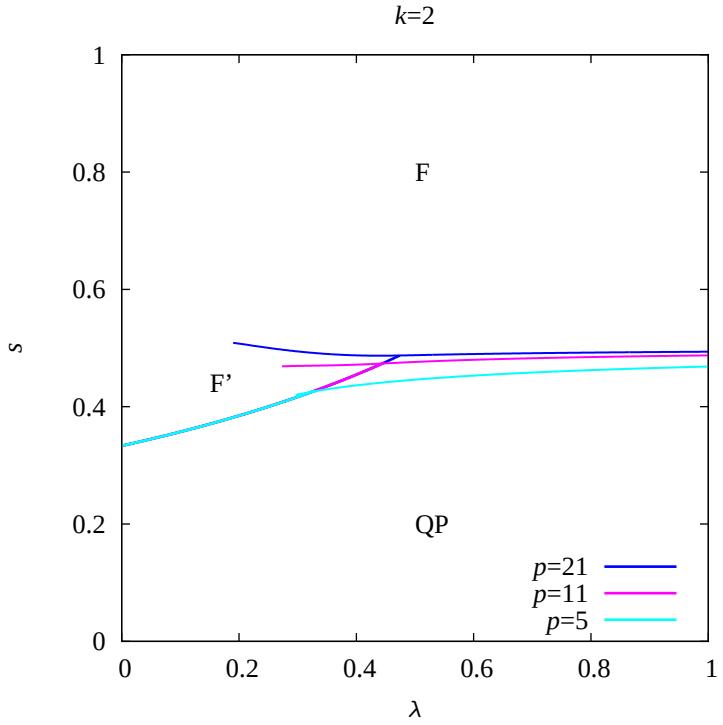

Figure 2. Phase diagram for $k = 2$. This is the same phase diagram as in reference [20]. The transition between the F' and QP phases is of second order, and the F-QP and F-F' transitions are of first order.

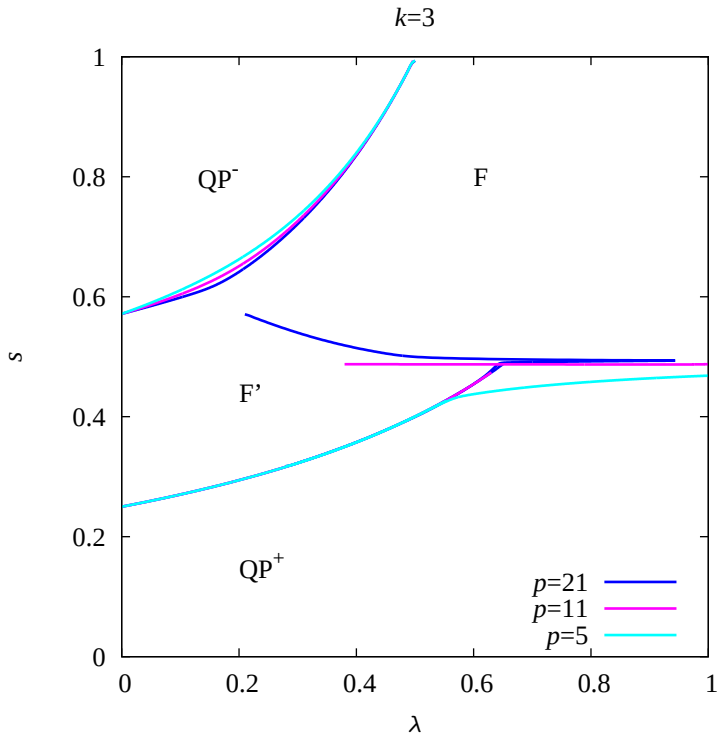

Figure 3. Phase diagram for $k = 3$. Only the F'-QP$^+$ transition is of second order.

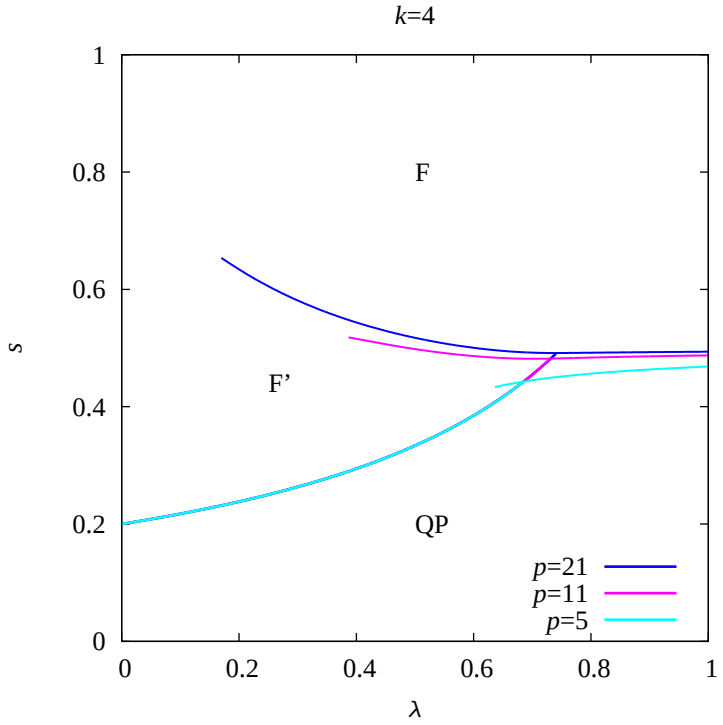

Figure 4. Phase diagram for $k = 4$. The structure is qualitatively the same as for $k = 2$.

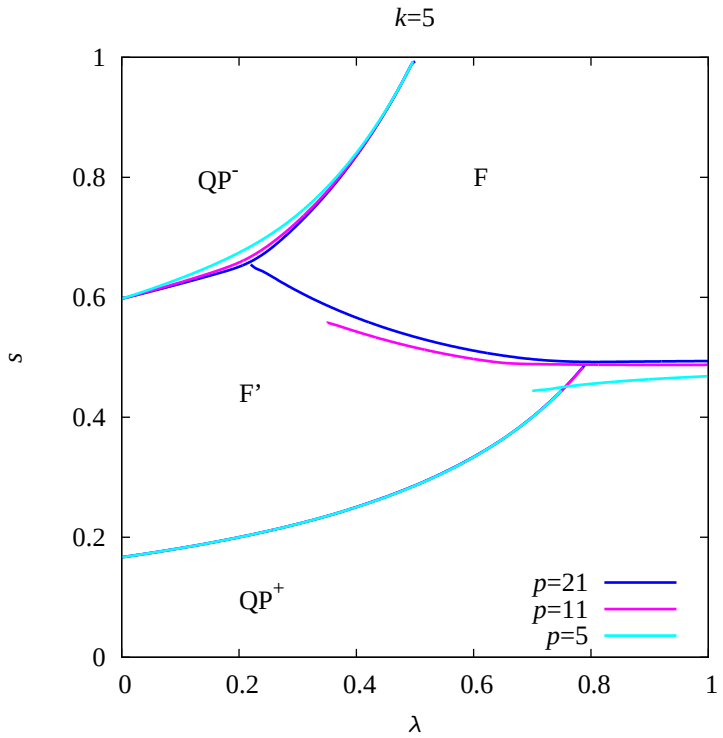

Figure 5. Phase diagram $k = 5$. The F'-QP$^+$ transition is of second order, and the other transitions are all of first order.

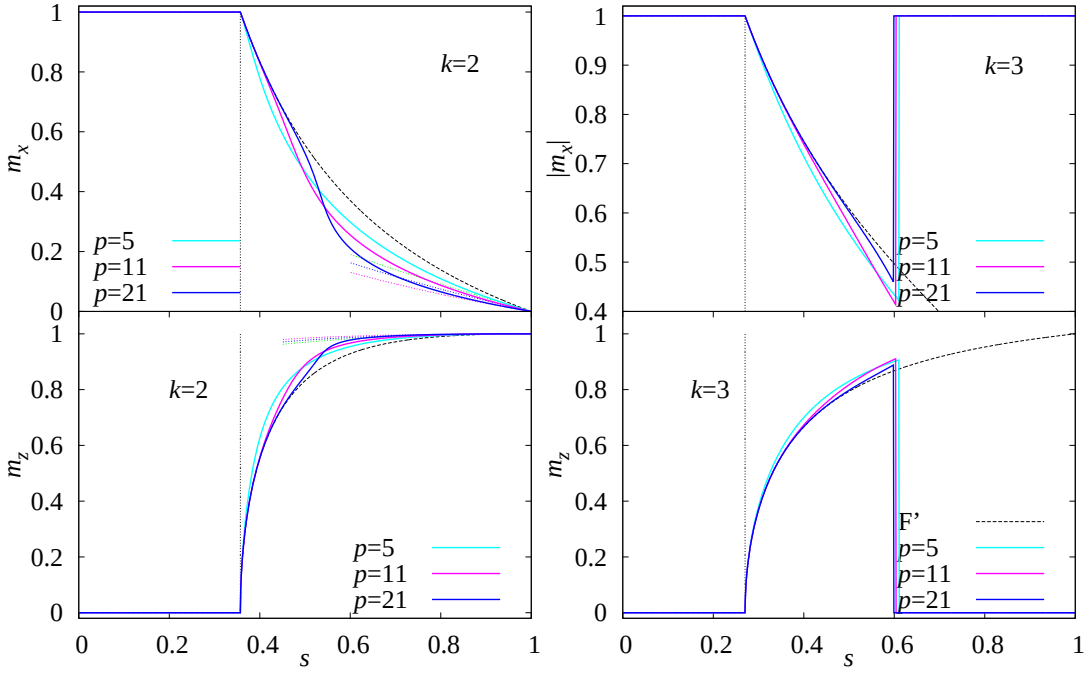

Figure 6. Magnetization obtained with the semi-classical approach as a function of s for $\lambda = 0.1$ and for $k = 2$ and 3. The dashed lines correspond to the analytical predictions for the QP$^{\pm}$, F (26) and F' (32) solutions.

magnetizations without crossing any transition on the way, see figure 6. However, when p is high and k is odd, transitions between the F and F' phases cannot be avoided, see figures 5, 6 and 7.

All this effect can be understood quantitatively coming back to the discussion of the $p \to \infty$ ferromagnetic solutions. Each of the phases were derived using the assumptions (16) for the F phase, and (21) for the F' phase. Now we discuss the validity of these approximations for p finite.

We begin with the F phase. This phase was obtained by introducing (16) in (13). Since this equality is not strictly true, we introduce it as an approximation $\sin^{p-2}\theta_0 \approx 1$, thus obtaining a new approximate equation

$$p\,s\,\lambda\cos\theta_0 + k\,s\,(1-\lambda)\cos^{k-1}\theta_0 - 1 + s \approx 0. \tag{25}$$

If we assume $\cos\theta_0 \ll 1$, the solution is

$$\cos\theta_0 \approx \frac{1-s}{s\,[p\,\lambda + k(1-\lambda)]}, \tag{26}$$

for $k = 2$, and

$$\cos\theta_0 \approx \frac{1-s}{s\,p\,\lambda}, \tag{27}$$

for $k > 2$. That means, that the F solution found for the $p \to \infty$ limit also appears for finite p whereas $\cos\theta_0 \ll 1$, or

$$\frac{1-s}{s\,p\,\lambda} \ll 1. \tag{28}$$

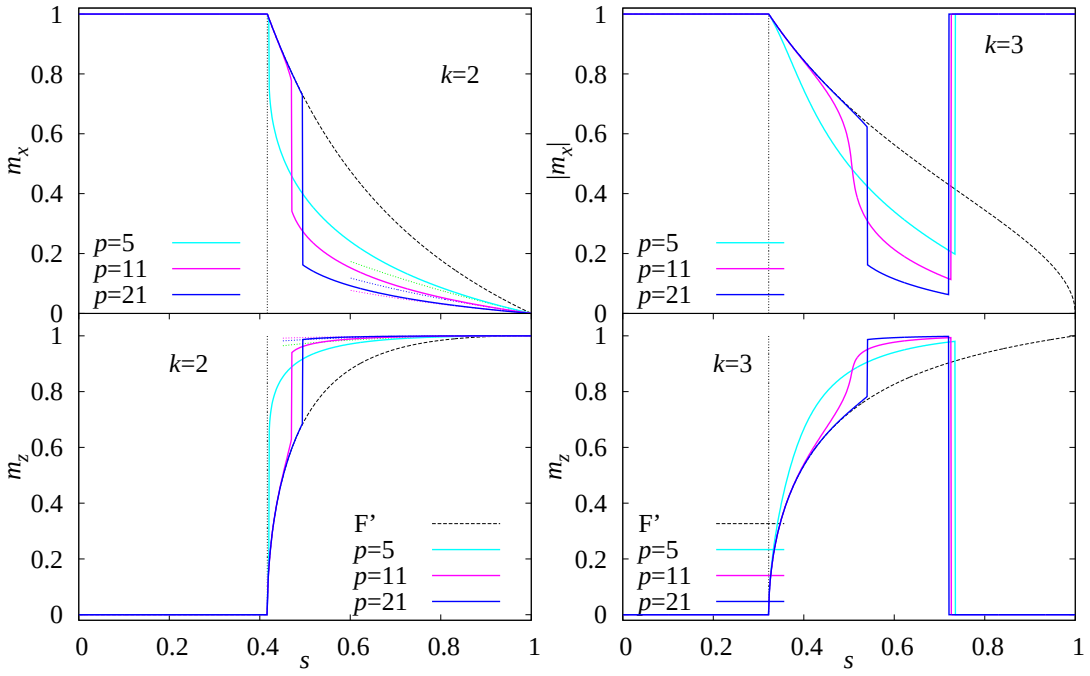

Figure 7. Magnetization obtained with the semi-classical approach as a function of s for $\lambda = 0.3$ for $k = 2$ and 3. The dashed lines correspond to the analytical predictions for the QP$^{\pm}$, F (26) and F' (32) solutions.

In particular, the smaller this quotient (28) is, the better approximation the F solution is. We can obtain the energies for finite p by introducing this solution in (11). For $k = 2$,

$$e_{\rm F}^{k=2}(s,\lambda) \approx -s\,\lambda\left[1-\left(\frac{1-s}{s\,[p\,\lambda+2\,(1-\lambda)]}\right)^2\right]^{\frac{p}{2}-1}$$
$$+s\,(1-\lambda)\left(\frac{1-s}{s\,[p\,\lambda+2\,(1-\lambda)]}\right)^k-(1-s)\left(\frac{1-s}{s\,[p\,\lambda+2\,(1-\lambda)]}\right), \qquad (29)$$

and for $k > 2$

$$e_{\rm F}^{k}(s,\lambda) \approx -s\,\lambda\left[1-\left(\frac{1-s}{s\,p\,\lambda}\right)^2\right]^{\frac{p}{2}-1}$$
$$+s(1-\lambda)\left(\frac{1-s}{s\,p\,\lambda}\right)^k-(1-s)\left(\frac{1-s}{s\,p\,\lambda}\right). \qquad (30)$$

Next we study the F' solution. We consider the following approximation

$$p\sin^{p-2}\theta_0 \approx 0. \qquad (31)$$

As before, if this is a good approximation,

$$\cos\theta_0 \approx \left[\frac{1-s}{k\,s\,(1-\lambda)}\right]^{\frac{1}{k-1}} \qquad (32)$$

is one solution to (13). This solution is equal to the one obtained for $p \to \infty$, (23). In other words, at this order of approximation, the solution is exact at this limit.

We briefly discuss the range of validity of this F' solution (32) for p finite. The approximation (31) is valid for small values of θ_0. With this idea we expand separately the two terms in (13) around $\theta_0 = 0$, the first term being

$$\sin^{p-2}\theta_0 \cos\theta_0 = p\, s\, \lambda\, \theta_0^{p-2} \left[1 - \frac{p+1}{6}\theta_0^2 + O(\theta_0^4)\right],$$

and the second term

$$\begin{aligned} & k\, s\, (1-\lambda) \cos^{k-1}\theta_0 - 1 + s \\ & = k\, s\, (1-\lambda) \left[1 - \frac{k-1}{2}\theta_0^2 + O(\theta_0^4)\right] - 1 + s. \end{aligned} \tag{33}$$

The dependency on θ_0 in the first term becomes irrelevant when $p > 3$, thus recovering the F' solution (32). When $p = 3$, the lowest power of θ_0 appears in the first term, leading to a different ferromagnetic solution, but not the F'. Clearly, the higher p (and the smaller θ_0) is, the better is approximation (31).

In general, for intermediate values of s and λ, the higher p is, the more exact the two ferromagnetic solutions, F and F', are. Then, since both approximations represent opposite cases in the value of m^x (or m^z), a new first-order transition between both phases will appear on the line when their two free energies become equal. However, for low values of p, or alternatively for $s \to 1$ or 0, there will only be one ferromagnetic solution, somewhere in between these two F and F' phases. This idea is well ilustrated in figures 6 and 7, where both the numerical solution to (13) and the analytical predictions (26) and (23) are displayed.

This has straightforward consequences on the performance of the quantum annealing algorithm: the higher p is, the narrower will be the region where annealing paths can avoid a first-order transition. In the limit of $p \to \infty$, as was discussed before, there will be only one possible path, but not effective as quantum annealing.

Concerning the transitions between the QP and ferromagnetic phases, we can distinguish two kinds of transitions. First of all, the transitions between the F and $\mathrm{QP}^{\pm}$ phases will be first order, since the F phase is characterized by a high value of m^z whereas the paramagnetic solution has $m^z = 0$. On the other hand, there is another transition between the F' and QP phases that lies on the line where their two free energies become equal, i.e. $s = 1/[1 + k(1-\lambda)]$. On this line, $m^x = 1$ ($m^z = 0$) for the two phases. Furthermore, the F' solution is exact for $m^x = 1$. Since the magnetizations are continuous on this line, the transition between F' and QP is of second order. Besides, it can be checked that there is a wide range of this line where $e_{\mathrm{F}'} < e_{\mathrm{F}}$. Thus, this phase is the stable one in the ferromagnetic phase. This second-order transition does not hamper the QA performance and gives us a way to avoid the F-QP phase transition that appeared when using the traditional QA approach. It is important to point out that this second-order transition appears for any value of k.

In Appendix A, we describe a different, quantum-mechanical method to derive the same results.

5. Energy gap

As discussed in Introduction, the efficiency of the QA algorithm is closely related to the behavior of the gap between the ground and first excited states. As usual, this gap can be computed by direct diagonalization of the problem Hamiltonian (7). Indeed, since the total spin $\boldsymbol{S}$ is conserved during the evolution, the dimension of the problem is $N+1$. That means that the diagonalization matrixes grow polynomially with the system size instead of exponentially as for generic quantum problems. However, still computer resources limit this computation to moderate sizes although such computations are useful for some purposes [20, 18]. Here, we adopt an alternatively approach, this gap can be computed in the thermodynamic limit $N \to \infty$ by the method described in [26]. The main idea is to extend the semi-classical scheme for the ground state by the consideration of quantum fluctuations around the classical ground state. It is important to point out that this method can only be applied in the case of finite gaps in the thermodynamic limit, as it is the case away from the transition points themselves. In case of exponentially small ones, other methods such as instantonic or WKB methods should be used [18, 21].

It is most convenient to rotate the system by an angle θ_0 around the y axis in order to bring the x axis parallel to the semi-classical magnetization, i.e.

$$\begin{pmatrix} S_x \\ S_y \\ S_z \end{pmatrix} = \begin{pmatrix} -\sin\theta_0 & 0 & \cos\theta_0 \\ 0 & 1 & 0 \\ \cos\theta_0 & 0 & \sin\theta_0 \end{pmatrix} \begin{pmatrix} \tilde{S}_x \\ \tilde{S}_y \\ \tilde{S}_z \end{pmatrix}. \tag{34}$$

We rewrite the Hamiltonian (8) in terms of these new variables $\tilde{S}^\alpha$, obtaining

$$\begin{aligned} \hat{H}(s,\lambda) = & -s\,\lambda\,N\left[\frac{2}{N}\left(\cos\theta_0\,\tilde{S}_x + \sin\theta_0\,\tilde{S}_z\right)\right]^p \\ & + s\,(1-\lambda)\,N\,\left[\frac{2}{N}\left(-\sin\theta_0\,\tilde{S}_x + \cos\theta_0\,\tilde{S}_z\right)\right]^k \\ & - 2\,(1-s)\left(-\sin\theta_0\,\tilde{S}_x + \cos\theta_0\,\tilde{S}_z\right). \end{aligned} \tag{35}$$

Now, we add quantum fluctuations to the system by means of the Holstein-Primakoff transformation

$$\tilde{S}_z = \frac{N}{2} - a^\dagger a, \quad \tilde{S}_+ = (N - a^\dagger a)^{1/2} a = \tilde{S}_-^\dagger, \tag{36}$$

where a is a boson annihilation operator that satisfies $[a, a^\dagger] = 1$. When quantum fluctuations are small relative to the classical state, i.e. for $N \gg \langle a^\dagger a \rangle$, we can use a simpler expression

$$\tilde{S}_x \approx \frac{\sqrt{N}}{2}(a + a^\dagger). \tag{37}$$

We introduce these transformations into the Hamiltonian (35) and expand the three different terms in powers of $1/N$. Thanks to the previous rotation, the coefficient in

$1/\sqrt{N}$ vanishes. We keep terms up to $1/N$ and group together all the coefficients with the same power of N. The result is

$$H(\gamma,\delta) = N\,e + \gamma + \gamma\left[(a^\dagger)^2 + a^2\right] + \delta a^\dagger a. \tag{38}$$

The term for N^1 is nothing but the ground energy obtained before in (11),

$$e \equiv -s\lambda \sin^p\theta_0 + s(1-\lambda)\cos^k\theta_0 - (1-s)\cos\theta_0. \tag{39}$$

The coefficients δ and γ are given as

$$\begin{aligned}\delta \equiv\ & -s\,\lambda\left[p(p-1)\sin^{p-2}\theta_0\cos^2\theta_0 - 2\,p\,\sin^p\theta_0\right] \\ & + s\,(1-\lambda)\left[k(k-1)\sin^2\theta_0\cos^{k-2}\theta_0 - 2\,k\,\cos^k\theta_0\right] + 2(1-s)\cos\theta_0,\end{aligned} \tag{40}$$

and

$$\gamma \equiv -\frac{s\,\lambda\,p(p-1)}{2}\sin^{p-2}\theta_0\cos^2\theta_0 + s\,(1-\lambda)\frac{k(k-1)}{2}\sin^2\theta_0\cos^{k-2}\theta_0 \tag{41}$$

We need to diagonalize this Hamiltonian in order to compute the first excited state by the Bogoliubov transformation

$$a = \cosh\frac{\Theta}{2}\,b + \sinh\frac{\Theta}{2}\,b^\dagger, a^\dagger = \cosh\frac{\Theta}{2}\,b^\dagger + \sinh\frac{\Theta}{2}\,b, \tag{42}$$

where b is a new bosonic annihilation operator satisfying $[b, b^\dagger] = 1$. Using this transformation, we can eliminate the coefficient of $\left[(b^\dagger)^2 + b^2\right]$ by choosing the angle Θ as

$$\tanh\Theta = -\frac{2\gamma}{\delta} \equiv \epsilon.$$

With this choice, the Hamiltonian can be written as

$$H(\gamma,\delta) = N\,e + \gamma + \frac{\delta}{2}\left(\sqrt{1-\epsilon^2} - 1\right) + \Delta\ b^\dagger b, \tag{43}$$

with

$$\Delta = \delta\sqrt{1-\epsilon^2}. \tag{44}$$

The Hamiltonian is diagonal in $b^\dagger b$. The energy gap in the $N\to\infty$ limit between the ground and first excited states is Δ.

Using the values θ_0 previously obtained solving (13), we can compute the energy gap for our system. We show the data for $p = 11$ and $\lambda = 0.1$ and 0.3 for different values of k in figure 8. As was suggested in the magnetization data in the previous section for $\lambda = 0.1$ (figures 2 to 5), no first-order transition F-F' is observed through the energy gap. The gap vanishes continuously on the second-order transition line but present no further jumps later, but the ones related to the F-QP$^-$ that always take place in the odd-k cases. On the contrary, when $\lambda = 0.3$, the jumps in the gap appear for all the k's at the place where we observed the F-F' transition before.

In the thermodynamic limit, the gap vanishes at a single point of first-order transition and remains finite away from this point. The single point of vanishing gap is hard to see by the present method, which results in an apparent simple jump in the gap at a first-order transition as seen in figure 8.

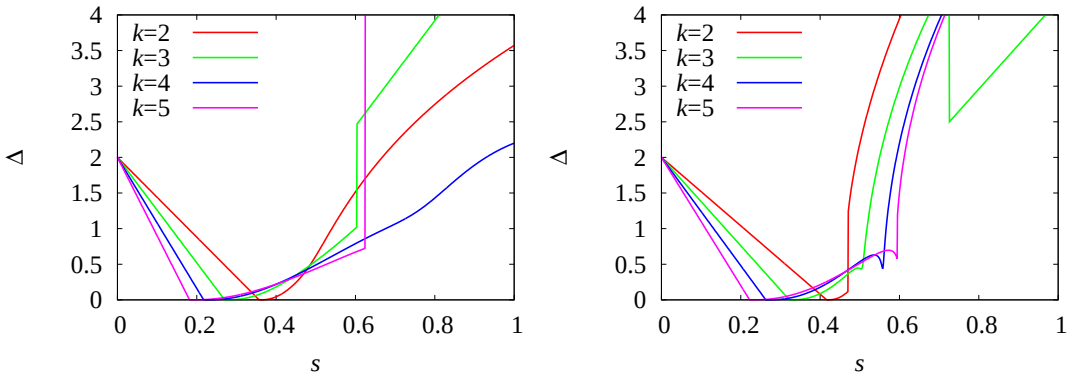

Figure 8. Energy gap for $p = 11$ as a function of s for $\lambda = 0.1$ (left) and $\lambda = 0.3$ (right) for several values of k.

6. Overlap of the ground-state wave functions

It has been suggested in [21] that the reason for the antiferromagnetic interaction, the $k = 2$ case in (6) introduced by Seki and Nishimori in [20], to work better than the transverse field interaction only is related to the large overlap between the ground states of the Hamiltonians $\hat{V}_{k=2}$ and $\hat{H}_0$. In this section, we will discuss the properties of these different states, concluding that, even thought the overlap is important, it is not the decisive factor that makes the strategy to succeed.

The ground state of $\hat{V}_{\rm TF}$ is the one where all the spins are aligned along the x axis, $|\phi_{\rm TF}\rangle = \otimes_{i=1}^{N} |\uparrow\rangle_i^x$. If we denote the ground state of $\hat{H}_0$, as $|\phi_0\rangle = \otimes_{i=1}^{N} |\uparrow\rangle_i^z$, the overlap between $|\phi_{\rm TF}\rangle$ and $|\phi_0\rangle$ decreases exponentially with N as 2^{-N}, as can easily be seen from the elementary relation $|\uparrow\rangle_i^x = \left(|\uparrow\rangle_i^z + |\downarrow\rangle_i^z\right)/\sqrt{2}$.

The overlap computation becomes a little more complicated for the ground state of $\hat{V}_k$. The ground state for this term depends on the value of k. Indeed, if k is odd, the ground state is the one where all the spins are aligned along the x axis, but towards the negative direction, i.e. $\otimes_{i=1}^{N} |\downarrow\rangle_i^x$. Then, the overlap with $|\phi_0\rangle$ for the k odd case will be exponentially suppressed as 2^{-N} as in the case of $\hat{V}_{\rm TF}$. Thus, the argument in [21] does not apply directly since we can avoid first-order transitions even in this case of k odd, in spite of the very small overlap of the ground state for $\hat{H}_0$ and $\hat{V}_k$.

The ground state for the k even case needs some care to be analyzed. We compute it in Appendix B. We show there that that the overlap is indeed higher for k even. The antiferromagnetic interations is a particular case, $k = 2$. In fact, the overlap displays an algebraic decay as the system size increases, i.e. $\sim 1/\sqrt{N}$.

We conclude that the overlap is not the main ingredient that makes the present method to succeed.

7. Conclusions

We have analyzed the reason for the failure of the traditional annealing with a transverse-field term in the infinite-range ferromagnetic p-spin model. We have shown that it is possible to find annealing trajectories that avoid the crossing of first-order transitions thanks to the introduction of a second driver term in the problem, which may be due to the multiple spin flips in the z-basis caused by the second term as was the case in [27]. This additional term favors the appearance of a second-order transition that does not hamper the annealing performance. A whole family of possible candidates has been studied and we conclude that the solution to the problem presented by Seki and Nishimori [20] is a special case of a more general additional quantum term. The main properties of these additional terms have also been discussed with the conclusion that the properties of the ground states of the diverse terms in the Hamiltonian are not a decisive factor to make the quantum annealing fail or succeed.

8. Acknowledgments

Beatriz Seoane was supported by the FPU program (MECD, Spain).

Note added in Proof: After the submission of the manuscript, it was pointed out that our Hamiltonians (4) and (6) were a special case of what was studied in [28, 29, 30].

Appendix A. Analysis with the Suzuki-Trotter formula

We investigate the properties of $\hat{H}(s,\lambda)$, the phase diagram in particular, using the decomposition formula [25] and the static approximation. This approach, although quantum, leads to the same results as the semi-classical method described in section 3. The method here is analogous to the one explained in detail in [20, 18], but we leave the power k as a free parameter in all the calculus. The purpose of this appendix is to confirm consistency between the method of the main text and that in [20, 18].

The starting point is the partition function,

$$Z = \mathrm{Tr}\, e^{-\beta \hat{H}(s,\lambda)}. \tag{A.1}$$

We use the decomposition formula to express it as

$$\begin{aligned} Z &= \lim_{M\to\infty} Z_M \equiv \lim_{M\to\infty} \mathrm{Tr}\left\{ e^{-\frac{\beta}{M} s\lambda \hat{H}_0} e^{-\frac{\beta}{M}\left[s\,(1-\lambda)\hat{V}_{\mathrm{AFF}} + (1-s)\hat{V}_{\mathrm{TF}}\right]} \right\}^M \\ &= \lim_{M\to\infty} \sum_{\{\sigma^z\}} \langle \{\sigma^z\}| \left\{ \exp\left[\frac{\beta s\lambda N}{M} \left(\frac{1}{N}\sum_{i=1}^{N} \hat{\sigma}_i^z \right)^p \right] \right. \\ &\quad \left. \times \exp\left[-\frac{\beta s\,(1-\lambda)N}{M} \left(\frac{1}{N}\sum_{i=1}^{N} \hat{\sigma}_i^x \right)^k + \frac{\beta(1-s)}{M} \sum_{i=1}^{N} \hat{\sigma}_i^x \right] \right\}^M |\{\sigma^z\}\rangle\,, \end{aligned} \tag{A.2}$$

where $\sum_{\{\sigma^z\}}$ refers to the summation over all the 2^N possible spin configurations in the z basis, and $|\{\sigma^z\}\rangle \equiv \otimes_{i=1}^{N} |\sigma_i^z\rangle$.

We introduce M closure relations, each one labeled by $\alpha(= 1, \ldots, M)$,

$$\hat{\mathbb{I}}(\alpha) \equiv \sum_{\{\sigma^z(\alpha)\}} |\{\sigma^z(\alpha)\}\rangle \langle\{\sigma^z(\alpha)\}| \times \sum_{\{\sigma^x(\alpha)\}} |\{\sigma^x(\alpha)\}\rangle \langle\{\sigma^x(\alpha)\}| , \tag{A.3}$$

just before the αth exponential operator involving $\hat{\sigma}_i^x$ in (A.2). The trace over the product of quantum operators is thus reduced to the product of numbers that commute and can be reordered,

$$\begin{aligned} Z_M = \prod_{\alpha=1}^{M} \sum_{\{\sigma^z(\alpha)\}} \sum_{\{\sigma^x(\alpha)\}} & \exp\left[\frac{\beta s \lambda N}{M}\left(\frac{1}{N}\sum_{i=1}^{N}\sigma_i^z(\alpha)\right)^p\right] \\ & \times \exp\left[-\frac{\beta s(1-\lambda)N}{M}\left(\frac{1}{N}\sum_{i=1}^{N}\sigma_i^x(\alpha)\right)^k + \frac{\beta(1-s)}{M}\sum_{i=1}^{N}\sigma_i^x(\alpha)\right] \\ & \times \prod_{i=1}^{N} \langle\sigma_i^z(\alpha)\,|\sigma_i^x(\alpha)\rangle \langle\sigma_i^x(\alpha)\,|\sigma_i^z(\alpha+1)\rangle , \end{aligned} \tag{A.4}$$

where $|\sigma_i^z(M+1)\rangle \equiv |\sigma_i^z(1)\rangle$.

We write the product in terms of the total x and z magnetizations in each copy of the system, i.e. $m^x(\alpha) \equiv \frac{1}{N}\sum_{i=1}^{N}\sigma_i^x(\alpha)$ and $m^z(\alpha) \equiv \frac{1}{N}\sum_{i=1}^{N}\sigma_i^z(\alpha)$, using the integral definition of the delta distribution

$$f\left(\frac{1}{N}\sum_{i=1}^{N}\sigma_i(\alpha)\right) = \int \mathrm{d}m\, \delta\left(m(\alpha) - \frac{1}{N}\sum_{i=1}^{N}\sigma_i(\alpha)\right) f\left(m(\alpha)\right). \tag{A.5}$$

After a few simplifications, we introduce the static approximation to remove the α dependence of the magnetizations. Under this approximation, we can compute the $M \to \infty$ limit using again the decomposition formula. The partition function (A.1) then reduces to

$$Z = \int \mathrm{d}m^z\, \mathrm{d}m^x\, \exp\left[-N\beta\, f(\beta, s, \lambda; m^z, m^x)\right], \tag{A.6}$$

where $f(\beta, s, \lambda; m^z, m^x)$ is the pseudo free-energy defined as follows:

$$\begin{aligned} & f(\beta, s, \lambda; m^z, m^x) = (p-1)\, s\, \lambda (m^z)^p - \,(k-1)\, s\,(1-\lambda)(m^x)^k \\ & -\frac{1}{\beta}\log\left\{2\cosh\beta\sqrt{\left[p\, s\, \lambda\,(m^z)^{p-1}\right]^2 + \left[1-s-s\,(1-\lambda)\,k\,(m^x)^{k-1}\right]^2}\right\} \end{aligned} \tag{A.7}$$

Again, one can apply the saddle-point method, obtaining two self-consistent equations for the two magnetizations,

$$\begin{aligned} m^z = & \frac{p\, s\, \lambda\,(m^z)^{p-1}}{\sqrt{\left[p\, s\, \lambda\,(m^z)^{p-1}\right]^2 + \left[1-s-s\,(1-\lambda)\,k\,(m^x)^{k-1}\right]^2}} \\ & \times \tanh\beta\sqrt{\left[p\, s\, \lambda\,(m^z)^{p-1}\right]^2 + \left[1-s-s\,(1-\lambda)\,k\,(m^x)^{k-1}\right]^2}, \end{aligned} \tag{A.8}$$

$$m^x = \frac{1-s-s\,(1-\lambda)\,k\,(m^x)^{k-1}}{\sqrt{\left[p\, s\, \lambda\,(m^z)^{p-1}\right]^2 + \left[1-s-s\,(1-\lambda)\,k\,(m^x)^{k-1}\right]^2}} \tag{A.9}$$

$$\times \tanh\beta\sqrt{\left[p\,s\,\lambda\,(m^z)^{p-1}\right]^2+\left[1-s-s\,(1-\lambda)\,k\,(m^x)^{k-1}\right]^2}.$$

In this work we are only interested in the purely quantum transitions, not in the thermodynamical ones. For this reason, and with the sake of simplification, we remove the dependence of physical quantities on β from now on by considering the low-temperature limit, $\beta\to\infty$. In this limit, if $\left[p\,s\,\lambda\,(m^z)^{p-1}\right]^2+\left[1-s+s\,(1-\lambda)\,k\,(m^x)^{k-1}\right]^2\neq 0$, the hyperbolic tangent in (A.8) and (A.9) tends to unity, and thus the self consistent equations simplify

$$m^z=\frac{p\,s\,\lambda\,(m^z)^{p-1}}{\sqrt{\left[p\,s\,\lambda\,(m^z)^{p-1}\right]^2+\left[1-s-s\,(1-\lambda)\,k\,(m^x)^{k-1}\right]^2}}, \tag{A.10}$$

$$m^x=\frac{1-s-s\,(1-\lambda)\,k\,(m^x)^{k-1}}{\sqrt{\left[p\,s\,\lambda\,(m^z)^{p-1}\right]^2+\left[1-s-s\,(1-\lambda)\,k\,(m^x)^{k-1}\right]^2}}. \tag{A.11}$$

The magnetization lies on the unit radius circumference, i.e. $(m^x)^2+(m^z)^2=1$. This result agrees with the approach in section 3, where the magnetization was a unit vector constrained to the XZ plane. The pseudo free energy (A.7) becomes

$$f(\beta,s,\lambda;m^z,m^x)=(p-1)\,s\,\lambda(m^z)^p-(k-1)\,s\,(1-\lambda)(m^x)^k$$
$$-\sqrt{\left[p\,s\,\lambda\,(m^z)^{p-1}\right]^2+\left[1-s-s\,(1-\lambda)\,k\,(m^x)^{k-1}\right]^2}. \tag{A.12}$$

Equations (A.10) and (A.11) have ferromagnetic (F) solutions with $m^z>0$ and quantum paramagnetic (QP) ones satisfying $m^z=0$ and $m^x\neq 0$. Let us begin with the latter case.

Appendix A.1. Paramagnetic solutions

Substituting $m^z=0$ in (A.11), we get

$$m^x=\frac{1-s-k\,s\,(1-\lambda)(m^x)^{k-1}}{\left|1-s-k\,s\,(1-\lambda)(m^x)^{k-1}\right|}, \tag{A.13}$$

which leads to $m^x=\pm 1$. The solution $m^x=-1$ is obtained if the numerator in (A.13) is negative, that is, if $1-s-k\,s\,(1-\lambda)(-1)^{k-1}<0$, which, in the range of parameters $0\leq s\leq 1$ and $0\leq\lambda\leq 1$ considered, can only be satisfied if k is odd and in the region $1/[1+k(1-\lambda)]<s\leq 1$. This phase is precisely the QM$^-$ phase discussed in the text. Its free energy is

$$f_{\mathrm{QP}^-}(s,\lambda)=1-2s+s\lambda, \tag{A.14}$$

which coincides with equation (15).

The other quantum paramagnetic solution with $m^x=+1$ (the QP$^+$ phase) can be satisfied only if the numerator is positive, i.e. if $1-s-k\,s\,(1-\lambda)\geq 0$, which can be fulfilled for any value of k as long as s lies in the region $0\leq s\leq 1/[1+k(1-\lambda)]$. The free energy of this phase is

$$f_{\mathrm{QP}^+}(s,\lambda)=-1+2s-s\lambda, \tag{A.15}$$

and is also equal to (14).

There is still one additional paramagnetic solution. In order to obtain it, we need to come back to the discussion about the $\beta \to \infty$ limit. The hyperbolic tangent in (A.8) and (A.9) could tend to a finite value in the $\beta \to \infty$ limit, as long as the term in the square root vanishes. Mathematically,‖

$$\lim_{\beta\to\infty} \tanh \beta \sqrt{\left[p\, s\, \lambda\, (m^z)^{p-1}\right]^2 + \left[1 - s - s\,(1-\lambda)\, k\, (m^x)^{k-1}\right]^2} = \tanh c, \quad \text{(A.16)}$$

when

$$m^z \to 0, m^x \to \left[\frac{1-s}{k\, s\, (1-\lambda)}\right]^{\frac{1}{k-1}}. \quad \text{(A.17)}$$

In order to find a non-trivial solution, it is also necessary in this limit that m^z tends to zero faster than the bracketed term of m^x in (A.9), i.e.

$$\frac{p\, s\, \lambda (m^z)^{p-1}}{1 - s - k\, s\, (1-\lambda)(m^x)^{k-1}} \to 0. \quad \text{(A.18)}$$

Under these assumptions, (A.8) and (A.9) imply $m^z = 0$ and $m^x = \tanh c$, where $\tanh c = [(1-s)/k\, s\, (1-\lambda)]^{\frac{1}{k-1}}$, in order to be consistent with the limit (A.17). This correspondence determines the region in the space where this phase can appear. In fact, as any hyperbolic tangent, $|\tanh c| \leq 1$, which is true only if $1/[1 + k\,(1-\lambda)] \leq s \leq 1$. Besides, the condition (A.18) forces $p > 3$.¶

Since the magnetization in the z direction vanishes, we call this phase QP2. The free energy is obtained with (A.7),

$$f_{\mathrm{QP2}}(s, \lambda) = -\frac{k-1}{k} \left[\frac{1-s}{k\, s\, (1-\lambda)}\right]^{\frac{1}{k-1}} (1-s). \quad \text{(A.19)}$$

This last phase was not predicted by the semi classical approach. However, we will see below that it is irrelevant to the problem, since the F' phase has always a smaller value of the free energy.

Appendix A.2. Ferromagnetic solutions

We next consider the possible solutions with $m^z > 0$.+ As before, the ferromagnetic solutions cannot be computed explicitly for a given value of p but for certain limiting cases.

‖ In the k-odd case, the limit

$$m^z \to 0,\ m^x \to -\left[\frac{1-s}{k\, s\, (1-\lambda)}\right]^{\frac{1}{k-1}}$$

also makes the square root in (A.16) vanish, but it leads to a positive free energy in (A.19), and thus it is not relevant.

¶ Indeed, using $(m^x)^2 + (m^z)^2 = \tanh^2 c = [(1-s)/k\, s\, (1-\lambda)]^{\frac{2}{k-1}}$ and computing the limit (A.17) when $m^x \to \tanh c$, one can check that it vanishes only as long as $p > 3$.

+ No negative value for m^z can satisfy (A.10) for odd values of p.

The solution $m^z = 1$ (and $m^x = 0$) is exact only on the line $s = 1$. However, we can see that an approximate solution $m^z \approx 1$ and $m^x \approx 0$ is valid in a wider space of parameters. Indeed, the solution

$$m^x = \frac{1-s}{s\,p\,\lambda}, \text{ and } m^z = \sqrt{1-\left(\frac{1-s}{s\,p\,\lambda}\right)^2} \tag{A.20}$$

fulfills (A.10) and (A.11) when $(1-s)/p\,s\,\lambda \to 0$. This is the F phase we obtained before in equation (30). The free energy is obtained plugging these values into equation (A.12). For the $p \to \infty$ limit,

$$f_{\mathrm{F}}(s,\lambda)|_{p\to\infty} = -s\lambda. \tag{A.21}$$

We consider an alternative solution for $0 < m^z < 1$. With this aim, we rewrite (A.10) in the following way

$$\left[(m^z)^2 - 1\right]\left[p\,s\,\lambda (m^z)^{p-1}\right]^2 + \left\{m^z\left[1 - s - s(1-\lambda)k(m^x)^{k-1}\right]\right\}^2 = 0. \tag{A.22}$$

In the $p \to \infty$ limit, $p(m^z)^{p-1} \to 0$, and

$$m^x = \left[\frac{1-s}{k\,s\,(1-\lambda)}\right]^{\frac{1}{k-1}} \quad m^z = \sqrt{1-\left[\frac{1-s}{k\,s\,(1-\lambda)}\right]^{\frac{2}{k-1}}} \tag{A.23}$$

is an exact solution to (A.22), and similarly of (A.11), as long as $(1-s)/k\,s\,(1-\lambda) < s \leq 1$, or $1/[1+k\,(1-\lambda)] < s < 1$.* This is precisely the F' phase discussed in section 3. Again, we compute the free energy by plugging the solution (A.23) in (A.12) and taking the $p \to \infty$ limit

$$f_{\mathrm{F}'}(s,\lambda)|_{p\to\infty} = -\frac{k-1}{k}\left[\frac{1-s}{k\,s\,(1-\lambda)}\right]^{\frac{1}{k-1}}(1-s), \tag{A.24}$$

which is exactly equal to the one obtained for the QP2 phase (A.19).

The solution (A.23) is also a good approximate solution for p finite (but $p > 3$) when $(m^z)^p \to 0$. The free energy for this phase is

$$f_{\mathrm{F}'}(s,\lambda) \approx -s\,\lambda\left[1-\left(\frac{1-s}{s\,k\,(1-\lambda)}\right)^{\frac{2}{k-1}}\right]^p - \frac{k-1}{k}\left[\frac{1-s}{k\,s\,(1-\lambda)}\right]^{\frac{1}{k-1}}(1-s), \tag{A.25}$$

which, for finite p, is always smaller than f_{QP2}. According to this observation, except for the $p \to \infty$ limit, the F' phase is always stabler than the QP2 phase.

We have therefore reproduced the results of section 3 by a completely different method. The present method is nevertheless better suited for generalizations to more complicate problems where the target Hamiltonian $\hat{H}_0$ cannot be expressed in terms of simple total spins.

* Again, the negative solution for m^x is also a valid solution in the odd k case but has a higher free energy than (A.23) due to the change of sign in the $(m^x)^k$ term in (A.12).

Appendix B. Ground state of $\hat{V}_k$ and its overlap with the ground state of $\hat{H}_0$

In this Appendix, we derive the properties of the ground state of $\hat{V}_k$ for k even. Let us first consider the case with N even. The ground state of $\hat{H}_0$, $|\phi_0\rangle = \otimes_{i=1}^{N} |\uparrow\rangle_i^z$, can be expressed as

$$\begin{aligned} |\phi_0\rangle &= \otimes_{i=1}^{N} \left(|\uparrow\rangle_i^x + |\downarrow\rangle_i^x \right)/\sqrt{2} \\ &= \frac{1}{2^{N/2}} \Big(|\uparrow\rangle_1^x |\uparrow\rangle_2^x \cdots |\uparrow\rangle_N^x + |\uparrow\rangle_1^x |\uparrow\rangle_2^x \cdots |\uparrow\rangle_{N-1}^x |\downarrow\rangle_N^x \\ &\quad + \cdots + |\downarrow\rangle_1^x |\downarrow\rangle_2^x \cdots |\downarrow\rangle_N^x \Big). \end{aligned} \tag{B.1}$$

This last expression has 2^N terms, in which the partial sum of terms with a half of the sites having $|\uparrow\rangle_i^x$ and the other half $|\downarrow\rangle_i^x$ is nothing but the ground state of $\hat{V}_k$ in the $S = N/2$ sector $|\phi_k\rangle$, up to a normalization,

$$\begin{aligned} |\phi_k\rangle &= a \Big(|\uparrow\rangle_1^x |\uparrow\rangle_2^x \cdots |\uparrow\rangle_{N/2}^x |\downarrow\rangle_{N/2+1}^x \cdots |\downarrow\rangle_N^x \\ &\quad + \cdots + |\downarrow\rangle_1^x |\downarrow\rangle_2^x \cdots |\downarrow\rangle_{N/2}^x |\uparrow\rangle_{N/2+1}^x \cdots |\uparrow\rangle_N^x \Big). \end{aligned} \tag{B.2}$$

It is easy to check from the number of terms in the above equation that the normalization condition is $a^2 \binom{N}{N/2} = 1$. We thus have

$$\langle \phi_0 | \phi_k \rangle = \frac{a}{2^{N/2}} \binom{N}{N/2} = \frac{1}{2^{N/2}} \sqrt{\binom{N}{N/2}}. \tag{B.3}$$

For large N,

$$\log | \langle \phi_0 | \phi_k \rangle |^2 = \log \left[2^{-N} \frac{N!}{\left(\frac{N}{2}!\right)^2} \right] \approx -\frac{1}{2} \log N + \log \sqrt{\frac{2}{\pi}}, \tag{B.4}$$

which means that the overlap decreases only polynomically with N as $\sim N^{-1/2}$.

The case of odd N can be analyzed similarly with $\binom{N}{N/2}$ replaced by $\binom{N}{(N+1)/2}$ or $\binom{N}{(N-1)/2}$.

References

[1] Papadimitriou C H and Steiglitz K 1998 *Combinatorial Optimization: Algorithms and Complexity* (New York: Dover)

[2] Garey M R and Johnson D S 1979 *Computers and Intractability* (San Francisco: Freeman)

[3] Mézard M, Parisi G and Virasoro M 1987 *Spin-Glass Theory and Beyond* (Singapore: World Scientific)

[4] Nishimori H 2001 *Statistical Physics of Spin Glasses and Information Processing: An Introduction* (Oxford: Oxford University Press)

[5] Barahona F 1982 *J. Phys. A: Math Gen.* **15** 3241

[6] Hukushima K and Nemoto K 1996 *J. Phys. Soc. Jpn.* **65** 1604

[7] Kirkpatrick S, Gelatt C D J and Vecchi M P 1983 *Science* **220** 671

[8] Kadowaki T and Nishimori H 1998 *Phys. Rev. E* **58** 5355

[9] Finnila A B, Gomez M A, Sebenik C, Stenson C and Doll J D 1994 *Chem. Phys. Lett.* **219** 343
[10] Das A and Chakrabarti B K 2008 *Rev. Mod. Phys.* **80** 1061
[11] Santoro G E and Tosatti E 2006 *J. Phys. A* **39** R393
[12] Farhi E, Goldstone J, Gutmann S, Lapan J, Lundgren A and Preda D 2001 *Science* **292** 474
[13] Hogg T 2003 *Phys. Rev. A* **67** 022314
[14] Young A P, Knysh S and Smelyanskiy V N 2008 *Phys. Rev. Lett.* **101** 170503
[15] Young A P and Knysh S 2010 *Phys. Rev. Lett.* **104** 020502
[16] Hen I and Young A P 2011 *Phys. Rev. E* **84** 061152
[17] Jörg T, Krzakala F, Kurchan J and Maggs A C 2008 *Phys. Rev. Lett.* **101** 147204
[18] Jörg T, Krazakala F, Kurchan J, Maggs A C and Pujos J 2010 *Europhys. Lett.* **89** 40004
[19] Jörg T, Krzakala F, Semerjian G and Zamponi F 2010 *Phys. Rev. Lett.* **104** 207206
[20] Seki Y and Nishimori H 2012 *Phys. Rev. E* **85** 051112
[21] Bapst V and Semerjian G 2012 *J. Stat. Mech.* P06007
[22] Grover L K 1997 *Phys. Rev. Lett.* **79** 325
[23] Roland J and Cerf N J 2003 *Phys. Rev. A* **68** 062312
[24] Grover L K 1996 *Proceedings of the 28th Annual Symposium on the Theory of Computing* (New York: ACM Press)
[25] Suzuki M 1976 *Prog. Theor. Phys.* **56** 1454
[26] Filippone M, Dusuel S and Vidal J 2011 *Phys. Rev. A* **83** 022327
[27] Suzuki S, Nishimori H and Suzuki M 2007 *Phys. Rev. E* **75** 051112
[28] den Ouden L, Capel H, Perk J and Tindemans P 1976 *Physica A* **85** 51
[29] den Ouden L, Capel H and Perk J 1976 *Physica A* **85** 425
[30] Perk J, den Ouden L and Capel H 1977 *Physica A* **89** 555